ELSEVIER

Sensors and Actuators B 87 (2002) 365–370

SENSORS AND ACTUATORS B CHEMICAL

www.elsevier.com/locate/sensorb

Enhancing the surface sensitivity of colorimetric resonant optical biosensors

Brian Cunningham*, Jean Qiu, Peter Li, Bo Lin

SRU Biosystems, 14A Gill Street, Woburn, MA 01801, USA

Accepted 19 July 2002

Abstract

Through alteration of the structure of a colorimetric resonant optical biosensor, the relative contribution of surface-binding effects to bulk refractive index effects can be influenced to favor detection of material in direct proximity to the sensor surface structure. The sequential buildup of polyelectrolyte monolayers has been used as a characterization method for determining the sensitivity of the device as a function of deposited thickness in an aqueous environment. A subtle change in the sensor structure is found to enhance surface sensitivity by ~4.5×.

Keywords: Optical biosensor; Proteomics; Micro-replication; Resonant filter; Direct assay

1. Introduction

Several optical biosensor approaches have been demonstrated which rely upon the detection of increased optical density caused by binding of biological material (for example: proteins, DNA, cells, bacteria) on a surface that has been activated with a receptor molecule [1–7]. Such sensors register a change in signal for any event that changes the optical density of the medium in contact with the sensor surface, whether it is from a biochemical-binding event or from a change in the ''bulk'' refractive index of the analyte solution. Most typically, an optical biosensor detects a combination of surface and bulk effects simultaneously. The bulk effect is subtracted from the measurement by referencing to a negative control surface that is known not to have adsorbed material present. The relative contribution of bulk and surface effects is determined by the spatial profile of the optical mode as it extends from the sensor surface into the test solution. Typically, an evanescent field extends from a planar sensor surface into the test sample with an exponentially decaying profile with a sampling distance on the order of hundreds of nanometers [8]. Only events occurring within the evanescent zone, whether surface or bulk effects, have the opportunity to influence the sensor measurement. Because biochemical interactions generally occur very close to the sensor surface (with dimensions of typical proteins ranging from 5 to 50 Å), it is of primary importance to have the highest sensitivity in the 500 Å region nearest to the sensor surface. Biochemical interaction with immobilized receptors generally is not occurring beyond this region, where bulk effects predominate.

In previous work, we have described a novel technology based upon a narrow bandwidth guided mode resonant filter structure that has been optimized to perform as a biosensor [9]. The sensor utilizes a sub-wavelength grating waveguide structure to provide a surface that, when illuminated with white light at normal incidence, reflects only a very narrow (resonant) band of wavelengths. The resonantly reflected wavelength is modified by the attachment of biomolecules to the waveguide, so that small changes in surface optical density can be quantified without attachment of a label to the detected biomolecule. Unlike optical detection approaches that rely upon interaction of detected molecules with an evanescent wave, the detection phenomenon in this work actually occurs *within* the waveguide, and thus provides for a strong interaction between surface-binding events and the transduced signal. Further advantages of the sensor approach are that the resonant reflected signal is measurable with the sensor either dry or immersed in liquid, and the simplicity of the non-contact excitation/detection instrumentation. Equivalent sensor structures have been fabricated onto glass substrates and incorporated into sheets of plastic film. Previous results demonstrate the ability to produce the biosensor in plastic over large surface areas and the incorporation of the

* Corresponding author. Tel.: +1-781-933-7255; fax: +1-781-933-5960.
E-mail address: bcunningham@srubiosystems.com (B. Cunningham).

0925-4005/02/$ – see front matter
PII: S0925-4005(02)00273-3

sensor into large area disposable assay formats such as microtiter plates and microarray slides [10].

Often, the sensitivities of optical biosensor detection technologies are compared by determining the minimum change in liquid bulk refractive index that can be resolved. This comparison technique is only useful when the surface and bulk sensitivities scale together, and does not reflect the fact that such sensors must be optimized to measure primarily surface effects. However, thorough characterization of sensor response as a function of distance from the sensor surface is difficult to perform, particularly within liquid media or under conditions that mimic protein binding that occurs during a biochemical assay.

In order to study the spatial-dependent sensitivity of the colorimetric resonant optical biosensor apart from the context of a biomolecular assay, experiments were performed in which a series of polyelectrolyte layers with defined thickness and refractive index are built on the surface. Previous researchers have identified this method as a reliable means for characterizing the surface sensitivity of optical biosensors without performing assays using immobilized protein receptor molecules. Because protein analytes are subject to the effects of surface capacity, binding conditions, and molecular orientation, polyelectrolyte deposition has been shown to be a more reliable means for obtaining a known amount of material on the sensor surface. A procedure for deposition of a sequence of positively and negatively charged polyelectrolyte films has been demonstrated as a means for reliably calibrating and comparing the response of various optical biosensors [11]. The polyelectrolyte multilayers behave as homogeneous and isotropic monolayers, while multilayers with proteins are expected to have more complex refractive index profiles.

In this work, we will use deposition of polyelectrolyte multilayers to evaluate and compare the bulk and surface contributions of two slightly different sensor designs. The results will show that a small change in sensor design can have a profound effect on the relative surface and bulk sensitivities, and that surface sensitivity of the biosensor has been improved substantially beyond values that have been reported previously. The results show that the surface and bulk sensitivity do not scale in the same proportion, and that it is possible to substantially reduce the relative contribution of bulk refractive index effects.

2. Materials and methods

2.1. Sensor design and fabrication

The sensor structure requires a grating with a period lower than the wavelength of the resonantly reflected light [12,13]. Structures reported in this work utilized a linear grating with a period of 500 nm and a depth of ~170 nm. As shown in Fig. 1, the grating structure is fabricated from a low refractive index material that is overcoated with a thin film of higher refractive index material. The grating structure was micro-replicated within a layer of cured epoxy on the surface of a polyester sheet, as described in previous research [9]. Fabrication is then completed by the deposition of a high refractive index dielectric thin film by sputter deposition. In the work reported here, two variations of the dielectric thin film structure were fabricated. One batch of sensors received sputter deposition of a ~120 nm thick layer of Ta_2O_5 directly on the cured epoxy grating surface. A second batch of sensors received a ~5 nm thick layer of SiO_2 directly on the cured epoxy surface, followed by the same Ta_2O_5 film received by the first batch. The SiO_2 film is referred to as a "tie layer" because it is intended to provide a transition region between the cured polymer material and the Ta_2O_5 film. In the experiments to follow, the two dielectric coating designs will be referred to as "no tie layer" and "tie layer."

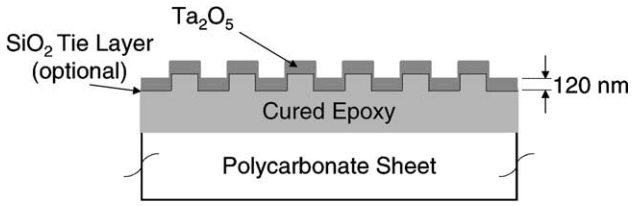

Fig. 1. Cross-sectional structure of the biosensor, showing the deposition of dielectric coating materials on the surface of the micro-replicated structure.

Following dielectric coating deposition, 3 in. × 5 in. microtiter plate sections were cut from the sensor sheet, and attached to the bottoms of bottomless 96-well microtiter plates (Greiner) with epoxy.

2.2. Polyelectrolyte multilayer process

The polyelectrolytes used in this study were anionic poly(sodium 4-styrenesulfonate) (PSS; M_W = 60,000 Da), cationic poly(allylamine hydrochloride) (PAH; M_W = 70,000 Da) and cationic poly(ethylenimine) (PEI; M_W = 60,000 Da). The polymers were purchased from Aldrich and used without further purification. The polyelectrolytes were dissolved in 0.9 M NaCl in HPLC water (filtered before use) at a concentration of 5 mg/ml. The 0.9 M NaCl solution is also used as buffer/rinse solution for the experiment. The buildup of the polyelectrolyte multilayer film is then realized by the following sequence of steps, during which the sensor is monitored at 10 s intervals:

(i) The 100 μl of 0.9 M NaCl buffer is pipetted into a microtiter well, and allowed to incubate on the sensor surface for 5 min to establish a stability baseline.
(ii) The buffer is removed, and 100 μl of PEI solution is added to the microtiter well, and allowed to incubate for 5 min.
(iii) The PEI solution is removed, and the well is rinsed with buffer. The sensor is monitored with buffer for 5 min.

(iv) PSS and PAH are alternately adsorbed on the PEI surface using the same procedure as described for PEI. A buffer rinse is used after every PSS and PAH incubation to re-establish a baseline for comparing net peak wavelength value (PWV) shifts without bulk solution effects. Progressively, a PEI–(PSS–PAH)$_n$ surface is deposited. A total of 35 polymer layers are deposited in sequence.

2.3. Readout instrumentation

In order to detect the reflected resonance, a white light source illuminates a ~1 mm diameter region of the grating surface through a 100 μm diameter fiber optic and a collimating lens at nominally normal incidence through the bottom of the microtiter plate. A detection fiber is bundled with the illumination fiber for gathering reflected light for analysis with a spectrometer (Ocean Optics). A series of eight illumination/detection heads are arranged in a linear fashion, so that reflection spectra are gathered from all eight wells in a microtiter plate column at once. The microtiter plate sits upon a motion stage so that each column can be addressed in sequence. For each measurement, a PWV is determined, and the PWV shift between two measurements is determined by subtracting the PWV of the sensor in a reference state (such as before an experiment begins) from the PWV of the sensor in its current state.

3. Results

3.1. Bulk refractive index sensitivity

The dependence of PWV on bulk refractive index was determined by placing droplets of different solvents on the sensor that span a wide range of refractive index (methanol, water, acetone, isopropyl alcohol, and glycerol) and recording the PWV. The PWV as a function of solution refractive index for the ''tie layer'' and ''no tie layer'' sensors is shown in Fig. 2 along with the bulk refractive index sensitivity of our first published sensor, which utilized an etched silicon nitride grating structure fabricated on a glass substrate [8]. In Fig. 2, all shifts are referenced to the PWV of the sensor immersed in methanol, which is defined as the ''zero'' PWV shift state. A linear fit was obtained for each sensor to determine the ''shift coefficient,'' $\sigma = \delta\text{PWV}/\delta n$, which is the slope of the linear fit. The bulk refractive index shift coefficient of the sensor without a tie layer was $\sigma = 270$, while the shift coefficient of the sensor with a tie layer was $\sigma = 158$. This result appears to indicate that the sensor without the tie layer is 1.7× more sensitive than the sensor with the tie layer included, and 3× more sensitive than the device fabricated on a glass substrate with a SiN dielectric grating ($\sigma = 89$).

3.2. Polyelectrolyte multilayer experiments

Using the protocol outlined previously, the PEI–(PSS–PAH)$_n$ multilayer was applied to the sensors while they were continuously monitored in the readout instrument for a total of $n = 17$ steps. Fig. 3 shows the progression of PWV as a function of time for the first three PSS–PAH layers. The PWV value for each layer was taken after washing with buffer solution, with the sensor exposed to buffer. Because the growth of each layer in the multilayer stack is self-limiting, previous research [11] has determined that the thickness of each layer is approximately 44 Å, and that the refractive index of the film is approximately $n = 1.49$. Using the buffer measurement after PEI injection as a reference baseline, the PWV shift for each subsequent buffer

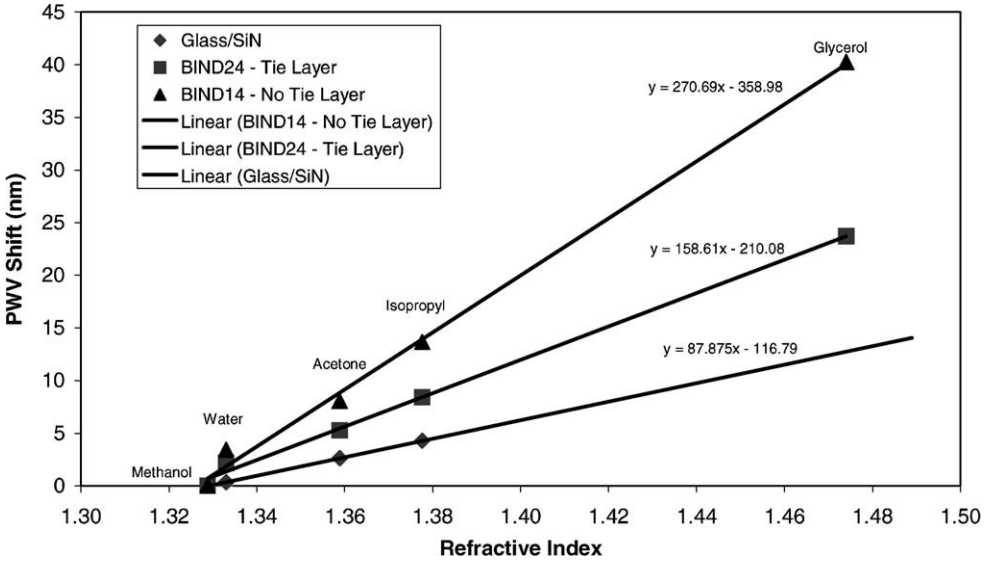

Fig. 2. Dependence of resonant peak wavelength value on the bulk refractive index of various liquids deposited on the surface. A linear fit is shown for each data set, and the bulk ''shift coefficient'' $\sigma = \delta\text{PWV}/\delta n$ is the slope of the line, where all PWV shifts are referenced against the PWV of the sensor in methanol.

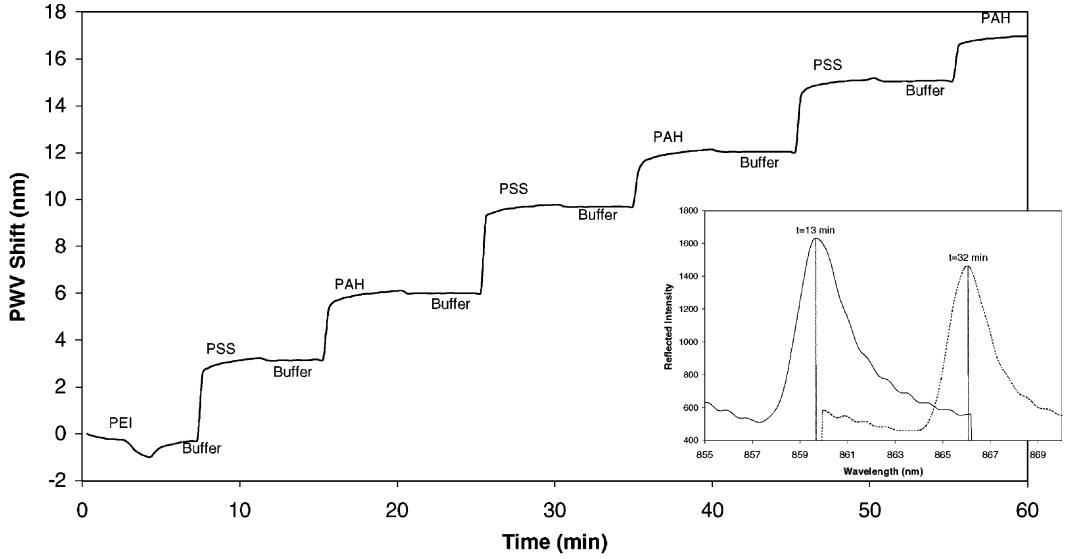

Fig. 3. The time course of the peak wavelength value as the first three (PSS–PAH) layers are deposited on the sensor surface. After the addition of each polymer, the sensor is rinsed with buffer solution to remove unbound material. The PWV of each step is measured with the sensor exposed to buffer. Each individual polymer layer (PSS or PAH) adds approximately 50 Å of material to the surface. Inset figure shows two reflectance spectra taken at different times during the course of the experiment.

measurement can be plotted as a function of total multilayer thickness, as shown in Fig. 4.

The sensor with the SiO_2 tie layer displays a nearly linear dependence of PWV with polymer thickness throughout the 1500 Å range while the sensor without the tie layer has a much stronger dependence of PWV on polymer thickness for the first ∼400 Å, which subsequently levels off until the two devices display approximately the same slope.

The differences between the two sensors can be understood more clearly by plotting the slope of the curves from Fig. 4 as a function of polymer thickness. Fig. 5 shows how the incremental sensitivity to additional polymer thickness (δPWV/δd) is roughly constant for the ‘‘tie layer’’ device, but is extremely thickness-dependent for the ‘‘no tie layer’’ sensor. Fig. 5 shows that the ‘‘no tie layer’’ sensor is ∼4.5× more sensitive for the first ∼200 Å of deposited material, but that the sensitivity advantage diminishes as one moves further away from the surface, until, after ∼700 Å of polymer is deposited, the ‘‘no tie layer’’ device actually becomes less sensitive than the ‘‘tie layer’’ device. Fig. 5 clearly shows the difference between a sensor that is optimized to measure predominantly surface-binding effects versus one that measures both surface and bulk effects with approximately equal sensitivity.

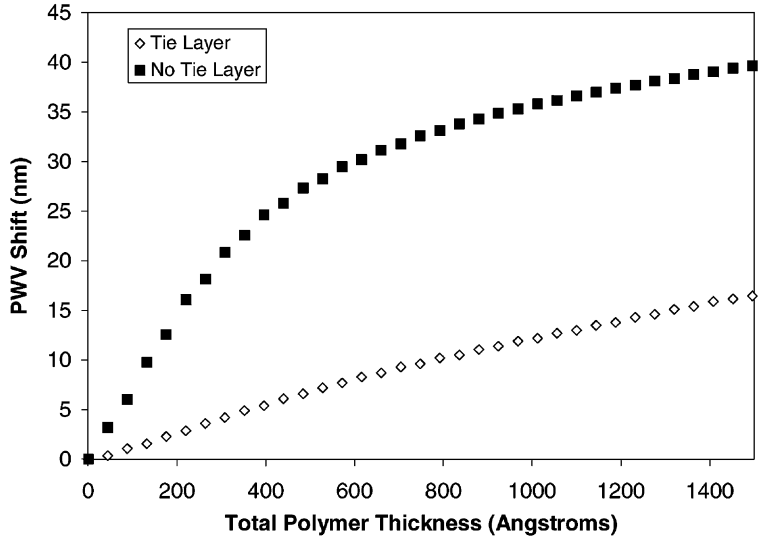

Fig. 4. Peak wavelength value as a function of polymer thickness for two dielectric coating designs. The data show that both sensors exhibit linear behavior at first, but that the ‘‘tie layer’’ sensor begins to show response saturation after 400 Å of material is deposited. However, the ‘‘no tie layer’’ sensor has substantially higher sensitivity for the first several polymer monolayers.

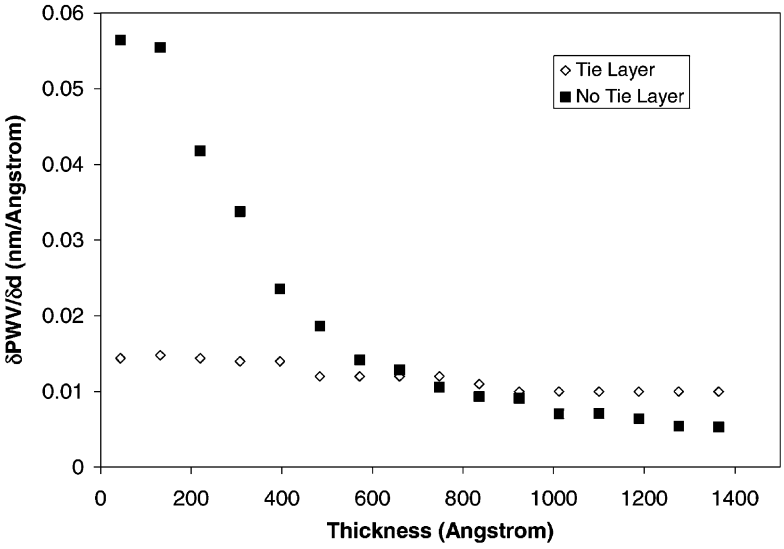

Fig. 5. The derivative of the thickness dependence of PWV as a function of polymer layer thickness. Each (PSS–PAH) group was considered as a single 100 Å-thick unit for the analysis. The sensor without a tie layer displays substantially higher sensitivity for the first ∼200 Å of polymer deposited, but eventually has less sensitivity for incremental thickness deposited greater than 700 Å.

4. Discussion

If deposition of polymer layers were to continue, one would expect that eventually $\delta\text{PWV}/\delta d$ would approach zero for both sensors, as the polymer thickness extends beyond the region where the optical field travels along the sensor surface. The curves in Fig. 5 were numerically integrated in order to compare the total integrated sensitivity of both sensor structures over their optical sampling depth. (The integral is computed by taking the sum of the $\delta\text{PWV}/\delta d$ values of Fig. 5 multiplied by 88 Å, so units are in nm.) The integral is intended to mimic how a bulk refractive index sensitivity comparison would be derived from the polyelectrolyte multilayer characterization method. Table 1 shows that the ratio of the integrals is close to the ratio of the bulk refractive index sensitivities, indicating that integration of the sensitivity roughly corresponds to the effect which occurs when the entire optical sampling depth is exposed to a bulk effect. Therefore, the bulk refractive index sensitivity combines the detection sensitivity of the entire optical sampling region of the sensor, without taking into account the proportion of the sensitivity derived from the region directly adjacent to the sensor surface (where biochemical binding generally takes place) to the sensitivity derived from regions a significant distance from the surface.

The large difference in performance between two similar sensor structures highlights the importance of considering the effect of seemingly innocuous dielectric materials on the distribution of optical modes within a surface waveguide-like device. Removal of the SiO_2 layer with a nominal refractive index of $n = 1.51$ and a thickness of only 50 Å had the effect of more tightly coupling lateral-traveling optical modes to the surface, thereby concentrating their energy more efficiently to the region where biochemical binding takes place. The mechanism of this dependence will be studied in future research, but is expected to involve not only the theoretically predicted effect of including tie layer with finite optical density, but also how the presence/absence of such layers impacts the abruptness of the transition region between the low and high refractive index materials within the sensor, and how the material and optical properties of the Ta_2O_5 layer are impacted by the morphology of underlying material.

Table 1
The numerical integral of the differential sensitivity curve (Fig. 5) was computed as a means for independently determining a bulk sensitivity coefficient from the polyelectrolyte multilayer data

	Tie layer	No tie layer	Ratio
Integral of differential binding curve (nm)	16.77	27.92	1.66
Bulk shift coefficient (nm)	158.61	270.69	1.71

The ratio of the coefficients of the two sensor types match closely to the ratios obtained from the bulk measurement (Fig. 2).

5. Conclusion

A polyelectrolyte multilayer characterization method has been used to study the relative contributions of surface and bulk effects on the PWV shifts measured on a colorimetric resonant optical biosensor. We have shown that it is possible to optimize the sensor structure through the design of the dielectric coating to substantially bias the sensitivity toward the sensor surface, thereby reducing the relative importance of bulk refractive index effects. We have also shown that sensor characterization based solely on the ability to detect

bulk refractive index differences does not adequately reflect the degree that sensitivity is dependent on the distance from the sensor surface. Because biochemical binding predominantly occurs in the near-surface region, this sensor design approach can be used to enhance the performance of optical biosensors.

Acknowledgements

The authors gratefully acknowledge John Gerstenmaier for performing the polyelectrolyte multilayer deposition experiments, and Brenda Hugh for fabrication of the sensors used in this work.

References

[1] R.E. Kunz, J. Edlinger, P. Sixt, M.T. Gale, Replicated chirped waveguide gratings for optical sensing applications, Sens. Actuators A 46/47 (1995) 482–486.
[2] P.M. Nellen, K. Tiefenthaler, W. Lukosz, Integrated optical input grating couplers as biochemical sensors, Sens. Actuators 15 (1988) 285–295.
[3] R. Cush, J.M. Cronin, W.J. Stewart, W.J. Maule, J. Molloy, N.J. Goddard, The resonant mirror: a novel optical biosensor for direct sensing of biomolecular interactions. Part I. Principles of operation and associated instrumentation, Biosens. Bioelectron. 8 (1993) 347.
[4] R. Jenison, S. Yang, A. Haeberli, B. Polisky, Interference-based detection of nucleic acid targets on optically coated silicon, Nat. Biotechnol. 19 (2001) 62–65.
[5] F.F. Bier, F.W. Scheller, Label-free observation of DNA-hybridisation and endonuclease activity on a waveguide surface using a grating coupler, Biosens. Bioelectron. 11 (6/7) (1996) 669–674.
[6] W. Huber, R. Barner, C. Fattinger, J. Hubscher, H. Koller, F. Muller, D. Schlatter, W. Lukosz, Direct optical immunosensing (sensitivity and selectivity), Sens. Actuators B 6 (1992) 122–126.
[7] W.A. Challener, J.D. Edwards, R.W. McGowan, J. Skorjanec, Z. Yang, A multilayer grating-based evanescent wave sensing technique, Sens. Actuators B 71 (2000) 42–46.
[8] A. Brecht, G. Gauglitz, Optical probes and transducers, Biosens. Bioelectron. 10 (1995) 923–936.
[9] B. Cunningham, P. Li, B. Lin, J. Pepper, Colorimetric resonant reflection as a direct biochemical assay technique, Sens. Actuators B 81 (2002) 316–328.
[10] B. Cunningham, B. Lin, J. Qiu, P. Li, J. Pepper, B. Hugh, A plastic colorimetric resonant optical biosensor for multiparallel detection of label-free biochemical interactions, Sens. Actuators B 85 (2002) 219–228.
[11] C. Picart, G. Ladam, B. Senger, J.-C. Voegel, P. Schaaf, F.J.G. Cuisinier, C. Gergely, Determination of structural parameters characterizing thin films by optical methods: a comparison between scanning angle reflectometry and optical waveguide lightmode spectroscopy, J. Chem. Phys. 115 (2) (2001) 1086–1094.
[12] R. Magnusson, S.S. Wang, New principle for optical filters, Appl. Phys. Lett. 61 (9) (1992) 1022.
[13] S. Peng, G.M. Morris, Resonant scattering from two-dimensional gratings, J. Opt. Soc. Am. A 13 (5) (1996) 993.